Cancer Chemother Pharmacol (1995) 36: 155–159

ORIGINAL ARTICLE

Edina Veszelovszky · Nicholas H.G. Holford
Lindy L. Thomsen · Richard G. Knowles
Bruce C. Baguley

Plasma nitrate clearance in mice: modeling of the systemic production of nitrate following the induction of nitric oxide synthesis

Received: 19 May 1994 / Accepted: 3 October 1994

Abstract Nitric oxide (NO) is produced in mammals by the enzyme NO synthase (NOS) in response to a number of agents, including the experimental antitumour agent flavone acetic acid (FAA) and the cytokine tumour necrosis factor-α (TNF). NO is converted rapidly in the presence of oxygen, water and haemoglobin to oxidation products, largely nitrate. To quantitate the production of nitric oxide it is necessary to know the clearance of nitrate. The concentration of nitrite and nitrate ion in the plasma of C_3H and BDF_1 ($C_{57}BL6 \times DBA_2$) mice was assessed before and after injection of sodium nitrate and sodium nitrite. Nitrite was converted rapidly to nitrate and the kinetics of elimination of nitrate were determined. There was no significant difference between results obtained with different mouse strains, between levels of nitrite and nitrate, or between i.p. and i.v. administration, and the observations were therefore combined. The volume of distribution of nitrate was 0.71 ± 0.04 l/kg and the clearance was 0.32 ± 0.02 $l/h^{-1}/kg^{-1}$ (plasma half-life, 1.54 h). Using previously published data, we developed a pharmacokinetic-pharmacodynamic model that relates the production of TNF in response to administration of FAA, the enhancement of NOS activity in response to TNF, and the elevation of plasma nitrate in response to NO production. This information permits the prediction from observed plasma nitrate values of the amount of NOS induced in vivo.

E. Veszelovszky · L.L. Thomsen[1] · B.C. Baguley (✉)
Cancer Research Laboratory, University of Auckland School of Medicine, Private Bag 92019, Auckland, New Zealand

N.H.G. Holford
Department of Pharmacology and Clinical Pharmacology, University of Auckland School of Medicine, Auckland, New Zealand

R.G. Knowles
Wellcome Research Laboratories, Langley Court, Beckenham BR3 3BS, UK

Present address:
[1] Wellcome Research Laboratories, Langley Court, Beckenham BR3 3BS, UK

Key words Plasma nitrate clearance · Nitric oxide · Nitric oxide synthase · Flavone-8-acetic acid · Tumour necrosis factor-α

Introduction

Nitric oxide (NO), as well as controlling aspects of the vascular, immune and central nervous system [19], has been found increasingly to play a role in tumour growth and in cancer chemotherapy. NO synthase activity in tissue from gynaecological cancer specimens is related to progression of the tumour [26]. Increased plasma nitrate concentrations in humans have been found following therapy with interleukin 2 [8, 20] and flavone-8-acetic acid (FAA) [24]. Increased plasma nitrate concentrations in mice are found in response to a number of antitumour agents such as bacterial endotoxin [4], tumour necrosis factor (TNF) [25] and the experimental antitumour agents FAA and 5,6-dimethylxanthenone-4-acetic acid [23].

NO is produced in mammalian cells through the oxidation of L-arginine by the enzyme nitric oxide synthase (NOS) [13]. At low concentrations it activates cell-regulatory enzymes such as guanylyl cyclase [10], whereas at higher concentrations it inactivates iron-containing proteins associated with respiration, leading to cytotoxicity [7]. NO reacts with water and oxygen to form approximately equal quantities of nitrite and nitrate [17]. The nitrite is in turn rapidly and irreversibly oxidised in blood to nitrate, which is then eliminated by excretion.

In the present study, we measured the pharmacokinetic parameters of plasma nitrate in mice following administration of nitrate and used these to develop a pharmacokinetic-pharmacodynamic model that describes both the kinetics of NOS activity and the total amount of NO produced in response to an appropriate stimulus. We extended this model to describe the relationship between the administration of FAA and the elevation of plasma nitrate. We used previously published observations describing the elevation of plasma nitrate in response to FAA [23] as well as the

elevation of TNF in response to FAA [16]. The model proposes physiological links between the concentration of FAA, the production of TNF, the induction of NOS and nitrate formation.

Materials and methods

Study design

FAA was supplied by the National Cancer Institute (USA). C_3H/HeN, C_3H/HeJ and DBA/2J × C57BL/6J F_1 hybrid mice were bred in the laboratory under institutional ethical guidelines and constant temperature, lighting and humidity [23]. Sodium nitrate was injected i.p. or i.v. at three doses (75, 250 or 750 μmol/kg) and plasma samples were prepared in triplicate either before treatment or at 0.25, 1, 2, 4, 6, 8, 12 and 24 h thereafter. Mice under ether anaesthesia were bled by cardiac puncture using heparinised syringes. Blood was centrifuged (1300 rpm, 5 min) to provide plasma samples. Plasma nitrate/nitrite concentrations were determined [23] by precipitation of plasma proteins with zinc sulphate, reduction with cadmium powder and colorimetric assay of the resulting nitrite with Griess reagent.

Model

The scheme that forms the basis of the model is shown in Fig. 1. The pharmacokinetics of plasma FAA, TNF, NOS activity (represented in the equations as NOS), NO and plasma nitrate (NO_3^-) were defined by a system of differential equations as follows:

$$dFAA/dt = -FAA \times CL_f/V_f, \quad (1)$$
$$dTNF/dt = RT_0 \times [1 + E_{faa}(FAA)] - TNF \times K_t, \quad (2)$$
$$dNOS/dt = RS_0 \times [1 + E_{tnf}(TNF)] - NOS \times K_s, \quad (3)$$
$$dNO/dt = NOS - NO \times K_{no}, \text{ and} \quad (4)$$
$$dNO_3^-/dt = (R_{no3,x} + R_{no3} - NO_3^- \times CL_{no3})/V_{no3}, \quad (5)$$

where CL_f and V_f are the clearance and volume of distribution of FAA, RT_0 is the synthesis rate of TNF prior to FAA treatment, $E_{faa}(FAA)$ is the fractional additional synthesis of TNF produced by FAA, K_t is the elimination rate constant of TNF. *NOS* is the activity of NOS, RS_0 is the synthesis rate of NOS associated with RT_0, $E_{tnf}(TNF)$ is the fractional additional synthesis of NOS produced by TNF, and K_s is the elimination rate constant of NOS. It is assumed that NOS induced by TNF has the same Michaelis constant as that of basal NOS. NO formation will be proportional to NOS at any constant substrate concentration (e.g. arginine) whether the synthase reaction is of the first or mixed order. K_{no} is the NO elimination rate constant and $R_{no3,x}$ is the infusion rate of exogenous nitrate. R_{no3} is the formation rate of NO_3^- from NO that is assumed to be identical to NO × K_{no}. The volume of distribution and clearance of NO_3^- after FAA administration was assumed to be the same as that estimated after exogenous nitrate. The elimination half-life of NO [ln(2)/K_{no}, including the conversion from nitrite to nitrate] is probably very short in relation to the time course of other events described by the model. The conversion of NO to NO_3^- can be considered instantaneous, such that R_{no3} is equal to NOS and, in fact, the predictions of the model were not substantively altered by assuming an NO elimination half-life of up to 0.1 h. The input rate of exogenous nitrate was modeled as a zero-order process lasting for 0.2 h. CL_{no3} and V_{no3} are the clearance and volume of distribution of NO_3^-.

The initial conditions of these equations were defined by the following relationships:

$$FAA_0 = Dose_{faa}/V_f, \quad (6)$$
$$TNF_0 = RT_0/K_t, \quad (7)$$
$$NOS_0 = (RS_0 \times [1 + E_{tnf}(TNF_0)]/K_s, \quad (8)$$
$$NO_0 = NOS_0/K_{no}, \text{ and} \quad (9)$$
$$NO_3{}^-{}_0 = NO_0 \times K_{no}/CL_{no3}. \quad (10)$$

If NOS_0 is assumed to be identical to the input rate of NO_3^- responsible for the pre-treatment NO_3^- concentration, then RS_0 can be identified.

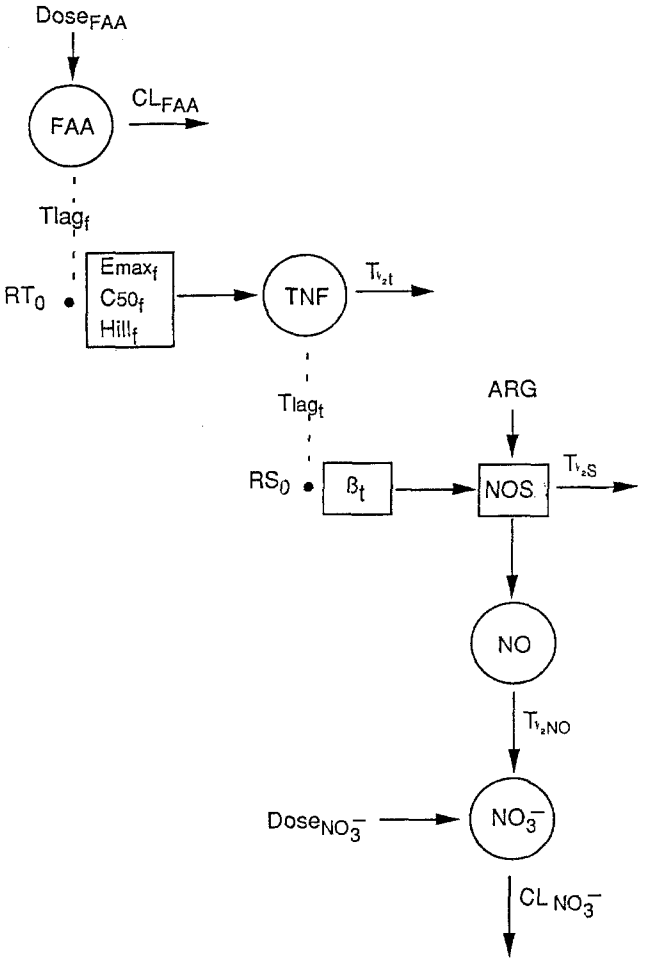

Fig. 1 Scheme showing the basis for the model described in Materials and methods and in Tables 1 and 2

The effect of FAA on TNF was substantially delayed in relation to plasma FAA concentrations. The time course of FAA at the presumed site of action on TNF synthesis was defined as FAA_e and was predicted using a lag time $Tlag_f$ as follows:

$$\text{If } t > Tlag_f \text{ then}$$
$$FAA_e = FAA(t\text{-}Tlag_f), \quad (11)$$
$$\text{Else } FAA_e = 0$$

The effect of TNF on NOS was also delayed in relation to the predicted TNF. A second lag time, $Tlag_t$, was introduced to account for this delay and predict the concentration of TNF at the site of action of NOS synthesis (TNF_e):

$$\text{If } t > Tlag_t + Tlag_f \text{ then}$$
$$TNF_e = TNF(t\text{-}Tlag_t\text{-}Tlag_f), \quad (12)$$
$$\text{Else } TNF_e = TNF_0$$

The effect of FAA_e on TNF synthesis was described by a sigmoid Emax pharmacodynamic model as follows:

$$E_{faa}(FAA_e) = Emax_f \times FAA_e{}^{Hillf}/(C50_f{}^{Hillf} + FAA_e{}^{Hillf}), \quad (13)$$

where $Emax_f$ is the maximal fractional increase in synthesis of TNF that can be produced by FAA, $C50_f$ is the concentration of FAA that produces 50% of the maximal effect and $Hillf$ is the Hill coefficient.

The effect of TNF_e on NOS formation was adequately described by a linear model as follows:

$$E_{tnf}(TNF_e) = \beta_t \times TNF_e, \quad (14)$$

where β_t is a slope parameter.

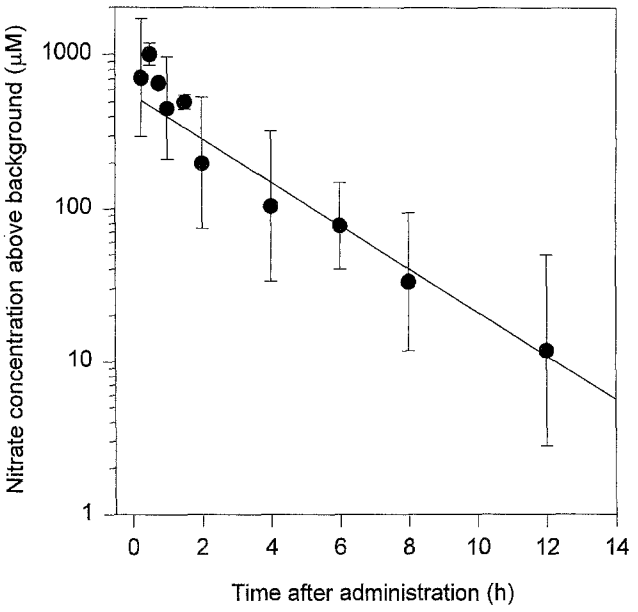

Fig. 2 Plasma nitrate concentrations (minus background plasma nitrate) detected in mice following administration of sodium nitrate at a dose of 750 μmol/kg. Data have been pooled for all three strains of mice and for i.v. and i.p. administration. *Vertical bars* represent standard deviations of data for each time point

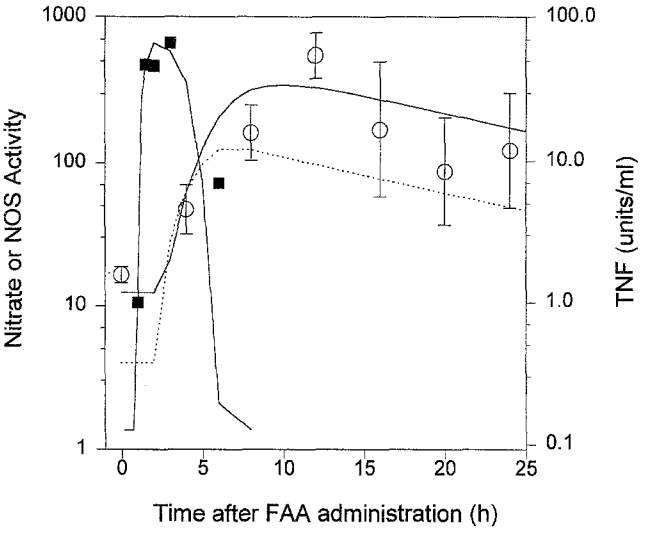

Fig. 3 Time courses predicted from the model for TNF, NOS (*dotted line*) and plasma nitrate following a single i.p. dose of FAA (1180 μmol/kg). Experimental points are shown for TNF (■) and nitrate (○). *Vertical bars* represent standard deviations for plasma nitrate determinations. The *dotted line* indicates NOS activity calculated from the model. Data on the *ordinate* are expressed in μmol h^{-1} kg^{-1} for NOS and in μ*M* for nitrate

Table 1 Pharmacokinetic parameters estimated for plasma nitrate after i.p. sodium nitrate administration at 750 mmol/kg

Parameter	Units	Value	SE
Nitrate distribution volume (V_{no3})	l/kg	0.71	0.04
Nitrate clearance (CL_{no3})	1 h^{-1} kg^{-1}	0.32	0.02
Residual error[a]	μ*M*	2.3	0.38
Basal NO_3^-concentration (NO_3^-0)	μ*M*	28.4	[b]

[a] Estimate of residual error (unexplained difference between observed plasma nitrate values and those predicted by the model) for each strain and dose group (indicated in brackets).
[b] Fixed parameter in the model.

The model was implemented using MKMODEL [9]. The differential equations were solved using Fehlberg's RKF45 method [5] with relative and absolute error tolerances of 10^{-6}. $Tlag_f$ and $Tlag_t$ could not be estimated directly but were adjusted manually to give a visually acceptable fit. Other data used for the model included the pharmacokinetics of FAA in BDF_1 mice [18], the induction of TNF in response to FAA [16] and the time course of plasma nitrate elevation in response to FAA [23]. We estimated the pharmacodynamic parameters of the model using these three sets of published observations together with the measurements of nitrate pharmacodynamics described in this report.

Results and discussion

The time course of plasma nitrate for up to 24 h after i.p. injection of sodium nitrate was measured. There was no significant difference between the results obtained with the three mouse strains or between i.v. and i.p. routes of administration. The data were therefore combined to estimate the pharmacokinetic parameters of injected nitrate in the mouse. The model used data for all doses of sodium nitrate and provided a mean plasma half-life of 1.54 h. Parameter estimates for exogenous nitrate administration are shown in Table 1. Data for one of the doses used (750 μmol/kg) are shown in Fig. 2. Injection of sodium nitrite (750 μmol/kg) produced results similar to those obtained using sodium nitrate at the same dose.

The time course of TNF and plasma nitrate after administration of FAA in tumour-bearing animals is shown together with the model predictions in Fig. 3. The parameter estimates for the full model after i.p. administration of FAA are listed in Table 2. A highly non-linear relationship between FAA concentration and TNF induction was observed, requiring a Hill coefficient of 20 to relate the TNF induction to FAA concentrations. This is consistent with the steep dose dependence of induction by FAA of both TNF production [16] and antitumour effects [22]. Standard error estimates are indicated in Table 2, although these cannot be used directly to determine confidence intervals on parameters estimated by non-linear regression [2]. The model provides an estimate of the total nitrate production in addition to that provided by basal nitric oxide synthesis and dietary intake of nitrate or nitrite. It thus estimates the additional total nitric oxide produced following a single dose (1190 μmol/kg) of FAA.

It is clear from the kinetics of induction of plasma nitrate that there is a considerable delay in its elevation following a single dose of FAA, necessitating the inclusion of two time delays in the model of 1 h for TNF response ($Tlag_f$) and 1 h for NOS response ($Tlag_t$). These may be justified firstly by assuming that NOS is induced not directly by FAA but rather through intermediate steps (in this case via the induction of TNF, which is itself delayed in relation to

Table 2 Pharmacodynamic parameters estimated from TNF and NO3-changes after administration of FAA at 1180 μmol/kg

Parameter	Units	Value	SE
FAAvolume of distribution (V_f)	l/kg	0.84	[b]
FAA clearance rate (CL_f)	1 h^{-1} kg^{-1}	0.13	[b]
Max. fractional stimulation by FAA ($Emax_f$)		476	289
FAA concentration causing 50% effect ($C50_f$)	μ*M*	781	383
TNF basal synthesis rate (RT_0)	units ml^{-1} h^{-1}	0.32	0.17
TNF half-life ($T1/2_t$)	h	0.27	0.14
Slope parameter (β_t)	μmol/kg	4.1	8.2
NOS basal synthesis rate (RS_0)	μmol h^{-1} kg^{-1}	0.16	0.25
NOS peak synthesis rate (NOS_{max})	μmol h^{-1} kg^{-1}	130	[b]
NOS half-life ($t_{1/2s}$)	h	11.2	6.0
Nitrate distribution volume (V_{no3})	l/kg	0.71	[b]
Nitrate clearance (CL_{no3})	1 h^{-1} kg^{-1}	0.32	[b]
Residual error (no3)	μ*M*	0.78	1.1
Residual error (tnf)[a]	units/ml	1.15	0.46
Basal TNF activity (TNF_0)	units/ml	0.13	[c]
Basal NO_3-concentration ($NO_3^-{}_0$)	μ*M*	12.4	[c]
Basal NO (NO_0)	μmol/kg	0.57	[c]
Basal generation of endogenous NO_3^- ($R_{no3,0}$)	μmol h^{-1} kg^{-1}	4.0	[c]

[a] Estimate of residual error (unexplained difference between observed values and those predicted by the model) for nitrate and TNF values
[b] Fixed parameters in the model
[c] Derived from initial conditions (Eqs. 6–10)

FAA administration) and secondly by assuming delays in the induction of TNF and NOS arising from gene expression and protein synthesis. The model assumes that TNF induces the NOS responsible for plasma nitrate elevation, since TNF is an inducer of NOS in many cells, including macrophages [11], hepatocytes [21] and endothelial cells [12, 15]. However, either other cytokines [3, 15] in addition to TNF or intermediate factors such as 5-hydroxytryptamine [1] may be involved in the induction of NOS.

The predicted time of maximal NOS in the model (5.7 h) is similar to that determined experimentally in rat liver (6 h) following endotoxin administration, which reached a peak after endotoxin treatment [14]. It is known that endotoxin induces TNF with kinetics comparable with those induced by FAA [6, 16] and that endotoxin induces plasma nitrate in rats with a time dependence similar to that observed with mice (L.L. Thomsen, unpublished results). The half-life of NOS was estimated as 11 h (Table 2) and accounts for the comparatively slow return of plasma nitrate towards pre-FAA treatment concentrations at between 6 and 24 h after FAA administration (Fig. 3). These data together with the model permit the prediction of the NOS rate at the time of peak plasma nitrate following any treatment (e.g. endotoxin, cytokines and cytokine-inducing agents). For example, a peak plasma nitrate concentration of 1000 μM is observed following treatment of mice with *Corynebacterium parvum* and is associated with a total liver NOS activity of 103 nmol/min (S. Moncada and D. Rees [22a] to L.L. Thomsen). The peak plasma nitrate can be used to calculate a total NOS rate of 320 μmol h^{-1} kg^{-1} (1000 μmol/l × 0.32 l h^{-1} kg^{-1} nitrate clearance), corresponding to 130 nmol/min in a 30-g mouse. Thus, the observed liver NOS activity is comparable with (but probably less than) the calculated whole-body NOS activity.

In conclusion, the pharmacokinetic data obtained for plasma nitrate in mice permit the pharmacodynamic analysis of host responses to endotoxin, cytokines and cytokine-inducing drugs such as FAA and 5,6-dimethylxanthenone-4-acetic acid. The mathematical model described herein provides a basis for the linking of further experimental data with biochemical mechanisms for the induction of NO synthesis and will facilitate the assessment of whole-body NO synthesis.

References

1. Baguley BC, Cole G, Thomsen LL, Zhuang L (1993) Serotonin involvement in the antitumour and host effects of flavone-8-acetic acid and 5,6-dimethylxanthenone-4-acetic acid. Cancer Chemother Pharmacol 3: 77–81
2. Bates DM, Watts DG (1988) Nonlinear regression analysis and its applications. Wiley, New York
3. Curran RD, Billiar TR, Stuehr DJ, Ochoa JB, Harbrecht BG, Flint SG, Simmons RL (1990) Multiple cytokines are required to induce hepatocyte nitric oxide production and inhibit total protein synthesis. Ann Surg 212: 462–471
4. Drapier J-C, Wietzerbin J, Hibbs JB (1988) Interferon-gamma and tumor necrosis factor induce the L-arginine-dependent cytotoxic effector mechanism in murine macrophages. Eur J Immunol 18: 1587–1592
5. Fehlberg E (1969) Low-order classical Runge-Kutta formulas with stepsize control and their application to some heat transfer problems. NASA technical report R-315. NASA, USA
6. Gifford GE, Flick DA (1987) Natural production and release of tumour necrosis factor. In: Bock G, Marsh J (eds) Tumour necrosis factor and related cytotoxins. (Ciba Foundation Symposia, vol 131) John Wiley and Sons, Chichester, pp 3–20
7. Hibbs JB Jr, Taintor RR, Vavrin Z, Granger DL, Drapier J-C, Amber IJ, Lancaster JR Jr (1990) Synthesis of nitric oxide from a terminal guanidino nitrogen atom of L-arginine: a molecular mechanism regulating cellular proliferation that targets intracellular iron. In: Moncada S, Higgs AE (eds) Nitric oxide from L-arginine: a bioregulatory system. Excerpta Medica, Amsterdam, pp 189–223
8. Hibbs JB, Westenfelder C, Taintor R, Vavrin Z, Kablitz C, Baranowski RL, Ward JH, Menlove RL, McMurry MP, Kushner JP, Samlowski WE (1992) Evidence for cytokine-inducible nitric oxide synthesis from L-arginine in patients receiving interleukin-2 therapy. J Clin Invest 89: 867–877
9. Holford NHG (1985) MKMODEL, a modelling tool for microcomputers – a pharmacokinetic evaluation and comparison with standard computer programs. Clin Exp Pharmacol [Suppl] 9: 95

10. Ignarro LJ (1992) Haem-dependent activation of cytosolic guanylate cyclase by nitric oxide – a widespread signal transduction mechanism. Biochem Soc Trans 20: 465–469
11. Keller R, Bassetti S, Keist R, Mulsch A, Klauser S (1992) Induction of nitric oxide synthase is a necessary precondition for expression of tumor necrosis factor-independent tumoricidal activity by activated macrophages. Biochem Biophys Res Commun 184: 1364–1371
12. Kilbourn RG, Belloni P (1990) Endothelial cell production of nitrogen oxides in response to interferon-gamma in combination with tumor necrosis factor, interleukin-1, or endotoxin. J Natl Cancer Inst 82: 772–776
13. Knowles RG, Moncada S (1994) Nitric oxide synthase in mammals. Biochem J 298: 249–258
14. Knowles RG, Merrett M, Salter M, Moncada S (1990) Differential induction of brain, lung and liver nitric oxide synthase by endotoxin in the rat. Biochem J 270: 833–836
15. Lamas S, Michel T, Brenner BM, Marsden PA (1991) Nitric oxide synthesis in endothelial cells – evidence for a pathway inducible by TNF-α. Am J Physiol 261: C634–C641
16. Mace KF, Hornung RL, Wiltrout RH, Young HA (1990) Correlation between in vivo induction of cytokine gene expression by flavone acetic acid and strict dose dependency and therapeutic efficacy against murine renal cancer. Cancer Res 50: 1742–1747
17. Marletta MA, Yoon PS, Iyengar R, Leaf CD, Wishnok JS (1985) Macrophage oxidation of L-arginine to nitrite and nitrate, nitric oxide is an intermediate. Biochemistry 27: 8706–8711
18. McKeage MJ, Kestell P, Denny WA, Baguley BC (1991) Plasma pharmacokinetics of the antitumour agents 5,6-dimethylxanthenone-4-acetic acid, xanthenone-4-acetic acid and flavone-8-acetic acid in mice. Cancer Chemother Pharmacol 28: 409–413
19. Moncada S, Palmer RMJ, Higgs EA (1991) Nitric oxide – physiology, pathophysiology, and pharmacology. Pharmacol Rev 43: 109–142
20. Ochoa JB, Curti B, Peitzman AB, Simmons RL, Billiar TR, Hoffman R, Rault R, Longo DL, Urba WJ, Ochoa AC (1992) Increased circulating nitrogen oxides after human tumor immunotherapy – correlation with toxic hemodynamic changes. J Natl Cancer Inst 84: 864–867
21. Pittner RA, Spitzer JA (1992) Endotoxin and TNF-α directly stimulate nitric oxide formation in cultured rat hepatocytes from chronically endotoxemic rats. Biochem Biophys Res Commun 185: 430–435
22. Plowman J, Naryanan VL, Dykes D, Szarvasi E, Briet P, Yoder OC, Paull KD (1986) Flavone acetic acid: a novel agent with preclinical antitumor activity against colon adenocarcinoma 38 in mice. Cancer Treat Rep 70: 631–638
22a. Rees DD, Cunha FQ, Assreuy J, Herman AG, Moncada S (1995). Sequential induction of nitric oxide synthase by *Corynebacterium parvum* in different organs in the mouse. Br J Pharmacol 114: 689–693
23. Thomsen LL, Ching LM, Zhuang L, Gavin JB, Baguley BC (1991) Tumor-dependent increased plasma nitrate concentrations as an indication of the antitumor effect of flavone-8-acetic acid and analogues in mice. Cancer Res 51: 77–81
24. Thomsen LL, Baguley BC, Rustin GJS, O'Reilly SM (1992) Flavone acetic acid (FAA) with recombinant interleukin-2 (rIL-2) in advanced malignant melanoma. 2. Induction of nitric oxide production. Br J Cancer 66: 723–727
25. Thomsen LL, Ching LM, Joseph WR, Baguley BC, Gavin JB (1992) Nitric oxide production in endotoxin-resistant C3H/HeJ mice stimulated with flavone-8-acetic acid and xanthenone-4-acetic acid analogues. Biochem Pharmacol 43: 2401–2406
26. Thomsen LL, Lawton FG, Knowles RG, Beesley JE, Riveros-Moreno V, Moncada S (1994) Nitric oxide synthase activity in human gynecological cancer. Cancer Res 54: 1352–1354